JOURNAL OF Materials CHEMISTRY

Lithium doped *N*-methyl-*N*-ethylpyrrolidinium bis(trifluoromethanesulfonyl)amide fast-ion conducting plastic crystals

Maria Forsyth,* Junhua Huang and Douglas R. MacFarlane

Department of Materials Engineering and Department of Chemistry, Monash University, Victoria, Australia 3800. E-mail: maria.forsyth@eng.monash.edu.au

Received 19th April 2000, Accepted 29th June 2000
First published as an Advanced Article on the web 23rd August 2000

The incorporation of dopant levels of lithium ions (0.5 to 9.3% by mole) in the *N*-methyl-*N*-ethylpyrrolidinium bis(trifluoromethanesulfonyl)amide (P_{12}TFSA) plastic crystalline phase results in increases in the solid state ionic conductivity of more than 3 orders of magnitude at 298 K. Conductivities as high as 10^{-4} S cm^{-1} at 323 K have been measured in these doped plastic crystal phases. These materials can therefore be classified as fast-ion conductors. Higher levels of Li only marginally increase the conductivity, up to around 33 mol%, followed by a slight decrease to 50 mol%. Thermal analysis behaviour has allowed the partial development of the binary phase diagram for the LiTFSA–P_{12}TFSA system between 0–50 mol% LiTFSA, which suggests the presence of a solid solution single phase at concentrations less than 9.3 mol% LiTFSA. There is also strong evidence of eutectic behaviour in this system with a eutectic transition temperature around 308 K at 33 mol% LiTFSA. A model relating ionic conduction to phase behaviour in this system is presented. The increased conductivity upon doping has been associated with lithium ion motion *via* ^{7}Li solid state NMR linewidth measurements.

Introduction

Plastic crystalline fast-ion conductors have been previously suggested as ideal candidates for solid-state lithium battery applications[1] due to their high single ion (or cation) mobility and their partly liquid like degrees of freedom which give the material deformable (plastic) mechanical properties. The other candidate electrolytes that have equally useful mechanical properties are, of course, the polymer-salt systems or polymer electrolytes,[2] however these materials suffer from low cation transport numbers. Plastic crystal phases[3] are so called because of their plastic mechanical properties, a feature which in most cases has its origins in the presence of rotational motions of the molecule (of one or both of the ions in an ionic plastic crystal phase). The rotating species or group remains localized in the crystalline lattice, however solid-state diffusion is observed[4] to be much higher in the plastic phase than in the underlying fully ordered phase. The enhanced diffusivities are thought to involve a vacancy diffusion mechanism. The onset of these rotational modes of motion are often marked by sharp thermal transitions in which a significant fraction of the overall enthalpy and entropy of fusion is involved, thus bringing the plastic phase thermodynamically much closer to the liquid phase. Timmermans[3] described these phases many years ago and proposed as an approximate characteristic the observation that the final entropy of fusion $\Delta S_f < 20$ J mol^{-1} K^{-1} for molecular plastic crystals. The plastic crystal phase of Li_2SO_4 is an example of a lithium fast ion conductor which has been extensively studied.[5] However, in the case of Li_2SO_4, the liquid like rotational degrees of freedom do not become active until above 773 K and hence this material is not suitable for low to medium temperature practical devices. In this system an anion rotation develops in the crystalline lattice above 773 K that is thought to enable the long range motion of the Li cation by a "paddle-wheel" type of mechanism. The implication therefore is that an ionic material, or a particular crystalline phase, which displays such rotational disorder is also likely to display high conductivities of one or more of the ions involved.

Other workers have also observed high diffusivities and plastic behaviour in certain families of organic compounds at considerably lower temperatures.[6–10] These reports have referred to the materials investigated as 'plastic crystals', 'mesophases' or 'rotator phases'. All of these descriptions have in common the need for rotational and/or translational disorder. It has been suggested that such disorder allows the creation of vacancies which leads to high diffusivities in the organic plastic crystal phase. Conductivity measurements have also been reported in tetraalkylammonium based salts and these show significant levels of ion conductivity in the plastic crystal phase.[9]

Recently as part of an investigation of the properties of organic salts[11] our group has reported[12,13] significant solid-state conductivities in a family of substituted pyrrolidinium bis(trifluoromethanesulfonyl)amide (TFSA) compounds (Scheme 1) . From the thermal analysis results it was evident that several solid–solid phase transitions were present in these materials. The entropies of fusion were generally in the region between 20 and 40 J mol^{-1} K^{-1}. This is in the vicinity of (although somewhat higher than) the Timmerman's criteria for plastic crystalline behaviour. However the deviation was rationalized in terms of the additional degrees of rotational freedom possessed by both ions in the compound, and the fact that the rotator phases may involve motions of only one of the ions. Thus it was concluded that the high conductivities were a direct result of plastic crystal behaviour produced by rotational disorder in these solids.

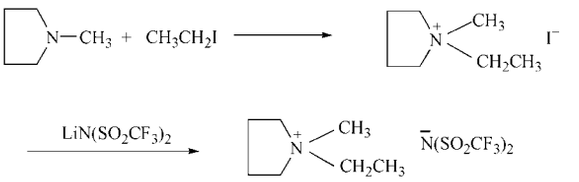

Scheme 1 Structure of *N*-methyl-*N*-ethylpyrrolidinium bis(trifluoromethanesulfonyl)amide

DOI: 10.1039/b003168m

A hypothesis that doping of lithium salts into these crystals would result in high lithium ion conductivities was subsequently tested and reported in a recent communication.[12] A 50 fold increase in conductivity over the undoped plastic crystal phase was reported with less than 1 mol% lithium ion dopant. Conductivities as high as 10^{-4} S cm^{-1} at room temperature were observed, suggesting that these doped materials should be considered as part of the broad family of fast-ion conducting materials.[1] This term is normally applied to a material in which there are rapid conductive motions of one (or more) ions within a, relatively, static crystalline or glassy matrix.

This paper discusses in more depth the relationship between phase behaviour and ion transport, in particular lithium ion mobility, in the *N*-methyl-*N*-ethylpyrrolidiniumTFSA–LiTFSA binary system over a range of compositions from the doped solid solution through to a 1 : 1 mol ratio mixture. This binary system has a common anion and a mixture of cations of very different shape and size; hence, it is hypothesized that the solid state mixtures are cation substituted or 'doped' analogues of the pure organic plastic crystal material over at least part of the binary composition range.

Experimental

Detailed preparation routes of the matrix materials used here have been described elsewhere.[13] The synthesis of *N*-methyl-*N*-ethylpyrrolidinium bis(trifluoromethanesulfonyl)amide (P_{12}TFSA)† is summarised in Scheme 1.

Samples were dried under vacuum prior to further use. A chosen amount (between 0.5 and 50 mol%) of lithium bis(trifluoromethanesulfonyl)amide (LiTFSA) (generously donated by 3M Specialty Chemicals Division, USA) was mixed with P_{12}TFSA to obtain a series of P_{12}TFSA–LiTFSA mixtures (all compositions are expressed as mol%). The mixtures were stirred at 100 °C for an hour and then allowed to cool to room temperature. The samples had the appearance of a waxy solid. All the samples were dried under vacuum at room temperature for at least three days before the thermal, electrical and NMR experiments were conducted.

Conductance measurements were carried out in locally designed multi-sample conductance cells which were made from a block of aluminium into which cylindrical sample compartments were machined with stainless steel outer and inner walls as the two electrodes. The temperature was measured by a thermocouple probe located in the aluminium block close to the sample compartment. The cell constant, *b*, of each compartment was obtained before and after each sample measurement by determining the capacitance of the empty cell. Cell constants were calculated *via*: $b = \varepsilon_0/C_0$ where ε_0 is the permitivity of free space and C_0 the empty cell capacitance. The cell constants were about 0.0025 cm^{-1}.

During the measurement, the cell was cooled using liquid nitrogen. The temperature was then ramped up at a steady rate of 0.2 °C min^{-1} under the control of a Shimaden Digital Temperature controller. Conductivity was obtained by measuring the complex impedance of the cell between 20 Hz and 1 MHz using a HP 4284A Impedance Meter. The conductance of the sample was determined from the real axis intercept in the Cole–Cole plot of the impedance data. Further details of the impedance analysis of these materials have been given elsewhere.[14]

The thermal properties were obtained by measuring about 10 mg samples contained in sealed aluminium pans using a Perkin-Elmer Model 7 Differential Scanning Calorimeter (DSC) at a heating rate of 20 °C min^{-1}. The range from 153 K to 523 K was obtained by measuring the samples over three smaller temperature ranges, from 153 K to 293 K, from 223 K to 323 K and from 293 K to 523 K.

^{7}Li linewidth measurements were performed on a Bruker AM-300 pulse NMR spectrometer operating at a Larmor frequency of 116.6 MHz. The 90-τ-180 and the 90-τ-90 pulse sequences were both used to acquire the data, where τ is the delay between the two pulses. Pulse lengths 90 and 180 were 5.3 s and 10.6 s, respectively. A τ value of 20 μs was used in all cases. Both pulse sequences gave similar central peak responses although the 90-τ-90 pulse sequence also clearly showed the quadrupolar peaks. Only the central transition is considered in this work. Relaxation delays from 50 s at about 170 K to 5 s at 360 K were employed. Spectra were typically accumulated for 16 scans at 170 K and 4 scans at 360 K. Short dead times of 10–30 μs were used to avoid loss of signal at early times. A peak simulation program package (Mac NMR) was used to fit the data.

Results and discussion

Thermal analysis

Typical thermal analysis scans are shown in Fig. 1 for a number of P_{12}TFSA–LiTFSA compositions ranging between 0 to 50.4 mol% LiTFSA. These measurements were usually performed in three different temperature regimes, as discussed previously, using the appropriate DSC apparatus. The pure P_{12}TFSA system shows an unusual shaped peak centred

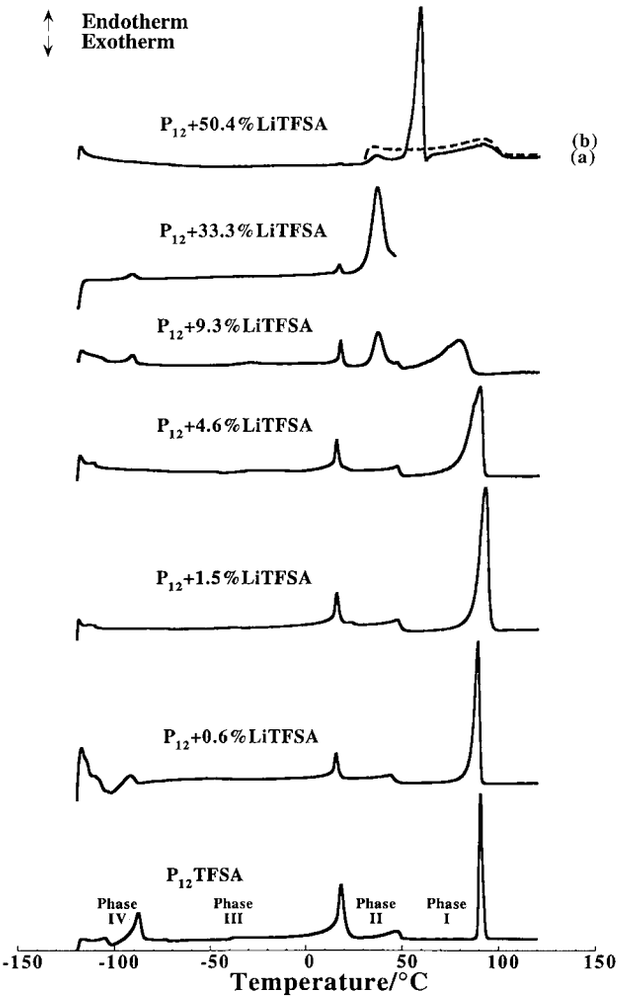

Fig. 1 Thermal analysis traces for P_{12}TFSA–LiTFSA mixtures at compositions indicated. Traces have been scaled for comparison of relative peak areas. Phase I to IV are indicated on the diagram.

†The shorthand nomenclature used for this compound (P_{12}) in our previous work has been supplemented with the acronym for the anion to become P_{12} TFSA. This is done to allow for a range of salts of other anions that have now been prepared.

around 181 K followed by a solid–solid transition which appears between 283 K and 289 K. The lower temperature exothermic transition is most likely due to a crystallization into what has been assigned as phase IV (using the phase nomenclature system of others[4]) followed by a phase IV to phase III transformation, as repeat scans often show the absence of the exothermic portion of the transition. It is interesting that the phase III to phase II transition at 284–289 K is reproducibly broad on the low temperature side possibly indicative of a slow transformation rate. In fact, the phase II to phase I transition at 314 K is similarly broad. Once again this unusual shape is completely reproducible in both the pure and mixed systems. Finally a sharp melting of phase I occurs at 363 K.

Dielectric and X-ray diffraction studies to be reported elsewhere suggest that Phase IV is probably the fully ordered phase. At higher temperatures the material passes through a series of phases exhibiting progressively greater disorder. The transition between these phases is not necessarily sharp (in which case they may not strictly be distinct phases), rather there is a progressive onset of the motions involved, in some cases culminating in a sharp completion and thereby a sharp trailing edge of the thermal analysis peak. Further analysis of the nature of these phases by X-ray diffraction is underway.

When 0.6% LiTFSA is doped into the P_{12}TFSA all the transitions remain approximately constant except for a broadening of the final melting, indicative of liquidus behaviour. An additional small peak is observed in the 1.5% Li doped system immediately following the phase III to phase II endotherm. This transition is variable in its appearance between 1.5% and 20% LiTFSA and may be related to metastable solid state behaviour. At compositions beyond 9% LiTFSA a further reproducible transition occurs at approximately 308 K ($\pm$3 K) as can be seen in Fig. 2. It should be noted that many of the observed transitions are highly dependent on the thermal history of the sample. In the case of the 33 mol% LiTFSA sample the final melting occurs at approximately 308 K and is quite sharp, indicative of a possible eutectic transition. To confirm that this is indeed a final melting, the sample has been visually confirmed to be a fluid liquid above 308 K. When this sample is quenched from the melt, a glass transition is observed and this 'eutectic' transition appears at lower temperatures following a devitrification exotherm; the low temperature crystallization process thus appears to produce a metastable phase in this case. Given the slow diffusion kinetics in solid state reactions, it is not unexpected to observe such a high degree of metastable behaviour.[15]

Fig. 2 presents a summary of the reproducible phase transitions as measured by DSC. This representation allows us to suggest possible phase behaviour. For example, it appears that a eutectic transition occurs at 308 K ($\pm$3 K) with a eutectic composition of approximately 33 mol% LiTFSA. In addition, a solid solution region is present at the low Li^+ content edge of the binary, with a maximum solubility of lithium ions in the P_{12}TFSA lattice of between 5 and 9.3 mol%. The data suggests that this solubility is dramatically decreased below the phase II $\rightarrow$ phase III transformation at 288 K. This is reminiscent of the phase behaviour of systems such as steel (Fe–C phase diagram) where the C is found in interstitial sites which are significantly larger in the austenitic phase (face centred cubic) as compared with the ferrite phase (body centred cubic). This decrease in interstitial volume in steel causes a solid–solid phase reaction, at the eutectoid, with the extra C rejected into the Fe_3C phase.[15] Given the relative sizes of the cations in this system (0.6 Å for Li^+ *versus* approximately 2–3 Å for P_{12}), it seems probable that the Li^+ ion will occupy interstitial sites. This is also more likely to satisfy its coordination requirements. It is possible that when Phase II transforms to Phase III, the interstitial sites or the vacancy sites significantly decrease in size and/or number such that lithium ion incorporation is not favoured. Further evidence of such changes are currently under investigation using Positron Annihilation Lifetime Spectroscopy (PALS) and X-ray Diffraction (XRD) techniques.

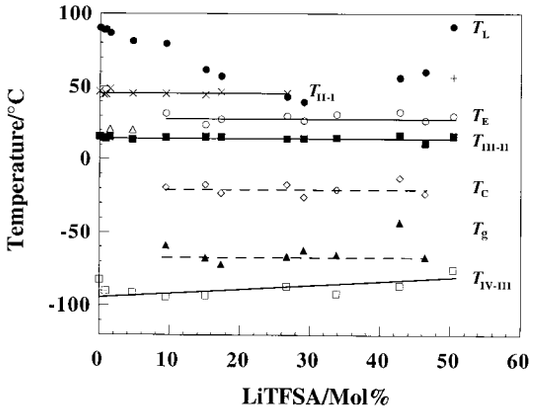

Fig. 2 Partial phase diagram for the P_{12}TFSA–LiTFSA binary, indicating apparently equilibrium solid–solid phase transitions (T_{IV-III}, T_{III-II}, T_{II-I}), glass transition temperature (T_g), devitrification temperature (T_C) and final melting temperature (liquidus, T_L). The apparent eutectic temperature T_E is also given.

The other significant feature of the phase diagram is the constancy of the P_{12}TFSA solid–solid phase transitions as a function of composition across the P_{12}TFSA rich region of the diagram, in particular the region of solid solution behaviour. This suggests that the solid solutions can be accurately considered to be Li^+ cation *doped* analogues of the pure P_{12}TFSA phase, exhibiting the same dynamic rotational disorder as the pure plastic crystal phases.

A further interesting behaviour in the phase diagram can be seen between about 10 mol% and 45 mol% LiTFSA, where a glass transition is regularly observed and always in the same temperature region, 213 K ($\pm$2 K). This is usually followed by a devitrification exotherm at 253 K ($\pm$10 K). The thermal data suggests that the phase changes in these mixed systems are kinetically slow and hence there is a tendency to become trapped in an amorphous state with subsequent devitrification into metastable phases. This could, of course, have significant impact on any devices that contained these materials as electrolytes and for which thermal cycling is likely.

Although compositions as high as 75 mol% LiTFSA have been investigated, the data is only discussed for samples up to 50 mol% LiTFSA due to the difficulty with reproducibility encountered for the higher compositions. Even at 50% we have observed unusual and variable behaviour. For example, in some traces it appears that a new, relatively sharp, symmetric peak is present at 330 K. A subsequent liquidus peak occurs at around 363 K for this composition; however, in some cases only the latter transition is observed. We postulate that the transition at 330 K may be associated with the formation of a new 1 : 1 compound such as that observed by Cooper and Angell in their 1 : 1 mix of $LiBF_4$ and (methoxyethyl)(dimethyl)-(ethyl)ammonium BF_4.[1] It should also be noted that in these higher LiTFSA compositions, the transition observed in the pure P_{12}TFSA at 314 K is no longer observed.

Conductivity analysis

Fig. 3(a) and (b) present temperature dependent ionic conductivity data for the LiTFSA–P_{12}TFSA system spanning the composition range from the pure P_{12}TFSA up to 50 mol% lithium salt and including a number of compositions in the doped region (up to 5 mol% LiTFSA). The Arrhenius format is used here (log conductivity *versus* inverse temperature) in order to readily compare activation energy changes with composition. The conductivity data presented here has been obtained

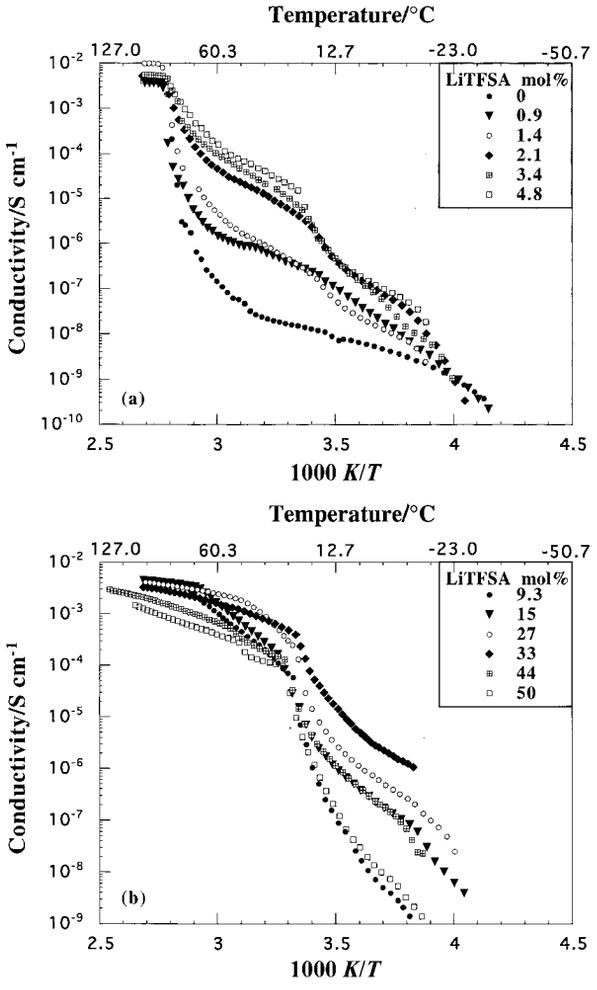

Fig. 3 Conductivity as a function of inverse temperature for (a) Li doped P_{12}TFSA systems (0→5 mol%) and (b) 9.3→50% mol% LiTFSA in P_{12}TFSA

from temperature dependent alternating current (ac) impedance analysis as previously described.[14] The observation of significant conductivity in the pure P_{12}TFSA well below the melting point has been reported in an earlier paper and has been associated with the disorder present in these 'plastic crystal' phases of this compound.[13] The rapid increase in the conductivity as a function of temperature by several orders of magnitude from 300 K up to the melting point can be rationalized as being either due to a rapidly increasing diffusion coefficient of the mobile ions or, alternatively, an increasing number of charge carriers. Both of these possibilities are consistent with an exponentially increasing number of vacancies; Ikeda and others have previously suggested that vacancies are responsible for conduction in this type of material.[4,9] The ^{7}Li NMR data is able to shed further light on this, as discussed further below.

The significant increase in conductivity observed at 300 K (almost two orders of magnitude) when less than 1 mol% LiTFSA is doped into the P_{12} phase must be associated with either a larger number of charge carriers or, more likely, the availability of significantly more mobile ions compared with the P_{12} cations. The slope $d\ln\sigma/d(1/T)$ in this solid state region appears smaller in the presence of the Li^+ dopant, which is consistent with a lower activation energy for conduction in the doped case. It is interesting to note that the conductivity at 315 K increases from 10^{-8} S cm^{-1} to 10^{-5} S cm^{-1} between 0 and 5 mol% LiTFSA, whereas higher concentrations of the lithium salt (up to 50 mol%) result in, at most, another order of magnitude increase in conductivity. Indeed at these higher concentrations the samples are heterogeneous, with at least part of the sample having melted at the eutectic transition (308 K). Thus one would expect both a higher mobility and a larger number of the mobile charge carriers (at any given temperature below the liquidus) as the Li^+ is increased towards the eutectic composition, since the volume fraction of the liquid phase increases. Above the eutectic composition the conductivity would then decrease as the concentration of LiTFSA increases. This is seen more clearly in Fig. 4, which presents the compositional dependence of the conductivity at a number of temperatures, both above and below the eutectic transition. The isothermal conductivity data indicates that highest conductivity is achieved at the eutectic composition (33 mol%), beyond which a decrease in the conductivity is seen.

Fig. 4 also allows a comparison of the conductivity changes below the various phase transition regions. For example, at 278 K the samples will be all solid, albeit a solid state mixture, and according to the phase diagram shown in Fig. 2, the stable P_{12}TFSA phase will be phase III. At this temperature, it appears that the lithium salt is less soluble in the P_{12} lattice (according to Fig. 2) and so the number of conducting lithium ions may be relatively small and not changing as more lithium salt is added to P_{12}TFSA. At the other extreme, when $T=368$ K, all samples are in the molten state and so it is not surprising that there is an insignificant compositional effect on the conductivity. If anything, the conductivity decreases with LiTFSA additions at 368 K, which can only be indicative of a decreasing ionic mobility since the number of charge carriers per unit volume is increasing slightly. This latter effect in the molten salt may simply be related to different degrees of ionic association in the melt.[16] In the phase II region, at 293 K, the conductivity is clearly seen to rise dramatically up to 5 mol% LiTFSA, whereas only smaller relative increases are seen beyond this point; eventually σ decreases again beyond the eutectic composition. In the phase I region, at 323 K, the increase is even more dramatic (4 orders of magnitude increase between 0 and 10 mol% LiTFSA) followed by a plateau in conductivity.

^{7}Li solid state NMR characterization

Given the importance of high lithium ion conductivity in solid-state lithium battery devices, it is important to ascertain whether or not the solid state conductivity observed in these doped and mixed systems can indeed be ascribed to the lithium ion. Our recent preliminary report on these systems presented ^{7}Li solid state NMR linewidth data as a function of temperature,[12] clearly showing that the line narrowing regions corresponded to phase changes observed by DSC. Furthermore the ^{7}Li linewidth in the solid state (below the eutectic temperature) was suggestive of liquid like translational motions (Figs. 5–7). These observations are expanded upon below.

Temperature dependent ^{7}Li NMR spectra for samples

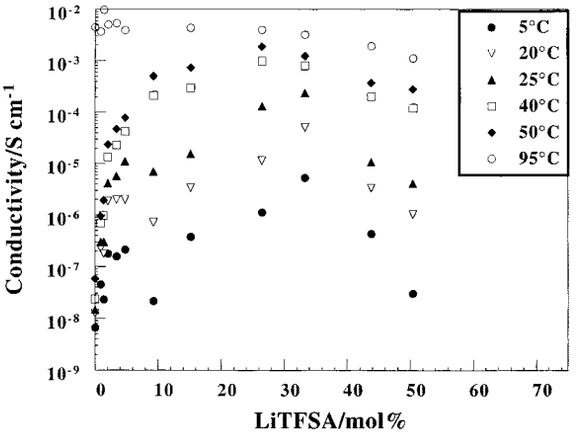

Fig. 4 Conductivity isotherms as a function of composition.

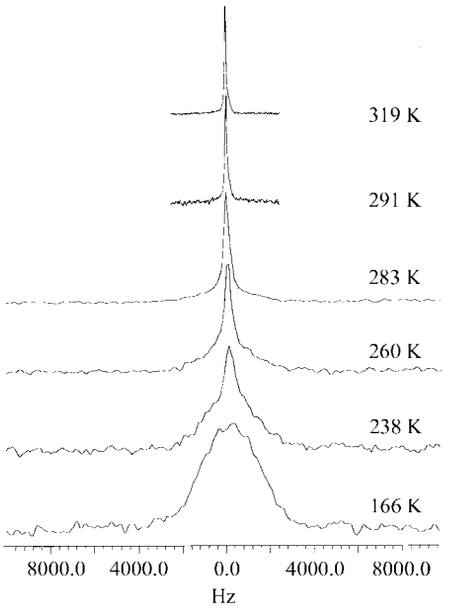

Fig. 5 ^{7}Li NMR spectra for 5 mol% LiTFSA samples as a function of temperature, spanning phase IV to phase I.

containing 5 mol%, 9.3 mol% and 33.3 mol% LiTFSA are presented in Figs. 5–7. At the lowest temperature, near 160 K, the spectra all display an apparently single, broad resonance with a linewidth of approximately 4000 Hz. This is typical of the rigid linewidth observed for lithium ions in other electrolyte systems, including polymer electrolytes in their glassy state,[17–19] and is indicative of the nature of the interactions for lithium species in these types of compounds. For example ^{7}Li–^{7}Li, ^{7}Li– ^{19}F or ^{7}Li–^{1}H dipolar interactions are all possible in this system just as they are in the typical polymer electrolytes.[20,21] With increasing temperature and above the phase IV to phase III transition, a second narrower line becomes evident. When peak simulation is used to fit the data, two peaks are required in all cases and an example of the results obtained from this fitting is given in Fig. 8 for the 5 mol% LiTFSA sample. The linewidth of this second peak is around 300 Hz, which is indicative of significant translational motion. Fig. 9 presents the area associated with each of the two peaks as obtained from the fitting. This relative area is at least qualitatively proportional to the concentration of observable lithium species and it can be seen that at 210 K, where the narrow ^{7}Li peak is first observed, the fraction of mobile species is about 2 orders of magnitude smaller than that of the immobile lithium species. However, a very dramatic rise in the concentration of this species is observed up to the temperature where the phase III to phase II transition occurs (approximately 289 K). This transition temperature also marks the point where significant line narrowing of both peak components occurs. Clearly the lithium ions in the phase II type P_{12}TFSA are significantly more mobile than in phase III. The data is also supportive of the hypothesis that lithium ions are significantly more 'soluble' in phase II compared with phase III, so that the decreasing linewidth and the rapidly increasing number of mobile species signifies an increased LiTFSA content in the solid solution of P_{12}TFSA–LiTFSA. Above about 312 K, the number of overall observable nuclei decreases, as would be expected from the temperature dependence of population distribution over the energy levels, resulting in an overall lower population of available/observable nuclei.[22] This is probably indicative of the fact that the solidus temperature (*i.e.* the temperature where the first liquid appears on heating) has been reached and beyond this temperature up to the final liquidus temperature (approx. 350 K), there will be both a doped solid and LiTFSA rich liquid phase present.

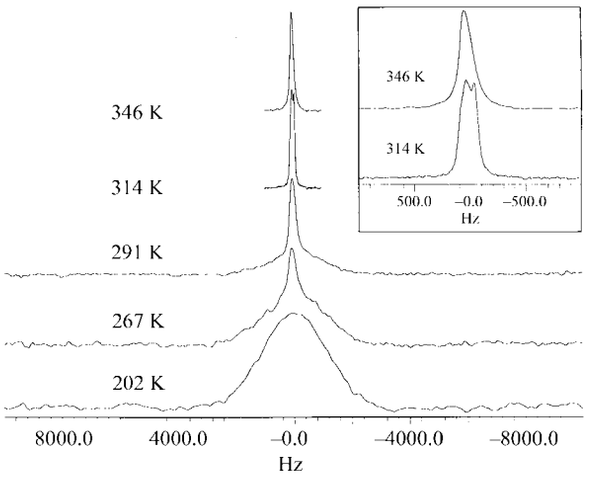

Fig. 6 ^{7}Li NMR spectra for 9.3 mol% LiTFSA samples as a function of temperature. The inset expands the frequency axis to clearly show the splitting above the eutectic temperature.

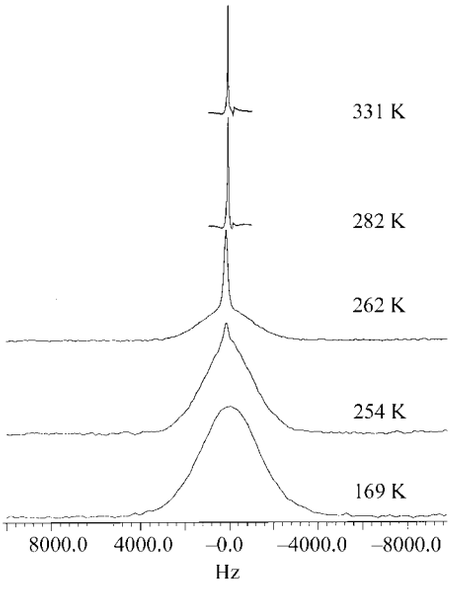

Fig. 7 ^{7}Li NMR spectra for 33 mol% LiTFSA samples spanning from phase IV up to the molten state.

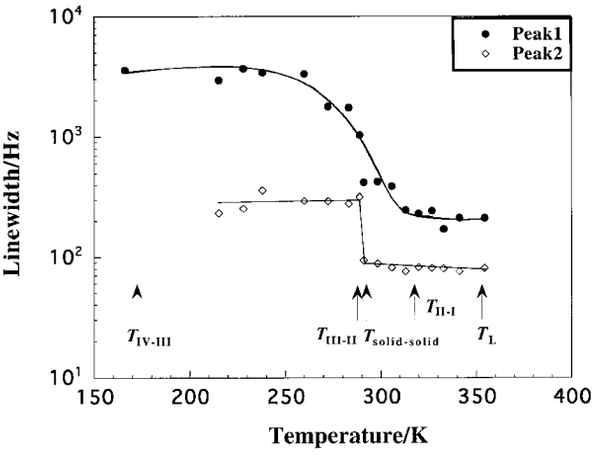

Fig. 8 ^{7}Li NMR full width at half maximum (FWHM) linewidths for 5 mol% LiTFSA as a function of temperature. The two lines were determined from simulations of the peak at each temperature. The various phase transitions are also indicated on this figure.

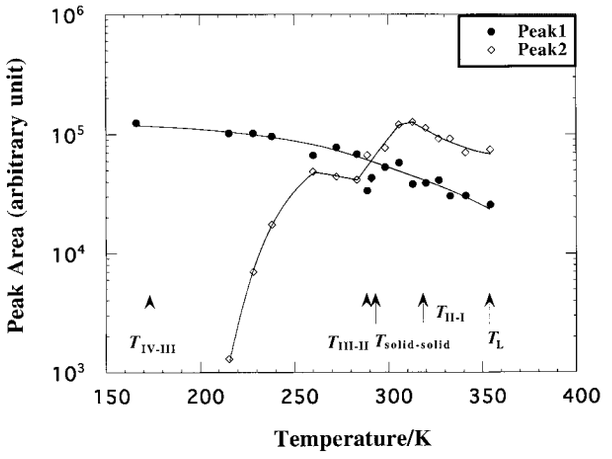

Fig. 9 ^{7}Li NMR peak areas as a function of temperature for the 5 mol% LiTFSA sample. The areas were determined from peak fitting to two peaks. The various phase transitions are indicated.

In the case of 9.3 mol% LiTFSA similar behaviour is observed at the lower temperatures, however, at temperatures beyond the eutectic transition (>308 K) two lithium peaks are clearly discernable. Both are narrow and the relative intensities change with increasing temperature until only a single narrow resonance is observed beyond the liquidus point where all species are in the melt. The two peaks which are observed in this high temperature case can be assigned to a liquid phase (the high field resonance) and a solid phase (low field resonance), the latter of which decreases in intensity as the final liquidus is approached. This assignment is confirmed by the data in Fig. 7 for the estimated eutectic composition (33 mol% LiTFSA) which shows a peak shift to higher frequencies when the eutectic temperature is reached. For this composition the change from solid to liquid occurs at a single temperature rather than over a range in temperatures, as expected for a eutectic composition.[15]

Conduction models

In related ionic plastic crystals described by Ono, Ikeda and coworkers,[6–10] significant diffusion of ions has been reported based on solid state NMR second moment and relaxation studies. The diffusivity was highest in the highest temperature phases; this was attributed to the increasing presence of lattice vacancies that occur as a result of the rotational disorder in the crystal. In the pure P_{12}TFSA material, the ionic conductivity is of the order of 10^{-8} S cm^{-1} over the temperature range 258 K to 323 K, beyond which the conductivity increases very dramatically up to 10^{-2} S cm^{-1} at the melting point. The phase II to phase I transition is complete at 319 K and hence the rapid upturn in conductivity may be associated with this transition. In the discussion that follows each phase region is discussed specifically with particular emphasis on the nature of the conduction process(es).

Phase III region. As lithium ions are doped into this P_{12}TFSA the apparent activation energy in phase III increases (as compared with pure P_{12}TFSA) and remains approximately constant independent of lithium ion concentration. The phase transformation data for this system indicates that, in all compositions studied, the materials are completely solid and beyond about 1.5% LiTFSA two solid phases are present a P_{12}TFSA rich phase and a LiTFSA rich phase. At this stage the second phase has not been isolated in its pure state and so it can not be confirmed whether or not this phase is responsible for conduction. What can be clearly observed from the conductivity data, however, is that higher conductivity occurs with higher lithium ion content in the phase III region of the temperature range up to 33 mol% and then the conductivity decreases once again. There are two possible explanations for this behaviour; the lithium ions doped in the P_{12}TFSA rich phase are significantly more mobile with increasing composition simply due to the decreasing liquidus temperature or the second, high lithium content phase, is also conducting. The similarity in the activation energies in this phase III region as a function of temperature is supportive of the first hypothesis. Chezeau and Strange[15] have clearly linked higher diffusivity to lower melting points in both metals and plastic crystals and, given a similar number of charge carriers, this would translate into a higher ionic conductivity for materials with lower melting points (or liquidus in the present system).

Phase II region. In the temperature range 288 K to 319 K two significant steps with composition can be seen both in activation energy behaviour and absolute conductivity. The first step is, as discussed earlier, a fifty fold increase in conductivity upon doping (<1.5% Li) the pure P_{12}TFSA. This occurs along with a slight increase in the activation energy in this temperature region. Further doping results in significantly higher conductivities, as well as higher activation energies. The ^{7}Li NMR for 5% and 9.3% LiTFSA showed that, in this temperature range, two types of lithium ions are present; a narrow, mobile species and a more rigidly bound species, as characterized by a broad ^{7}Li linewidth. Also in this temperature range and beyond the eutectic transition, a liquid phase will now be present which must also contribute to the conductivity. Interestingly, there does not appear to be any sudden change in the conductivity at this transition temperature, again indicating the high mobility of the lithium ions doped in the phase II P_{12}TFSA lattice. The NMR on the other hand was able to clearly show two distinct narrow lines in the 9.3% sample, one of which was associated with the melt and the other with the conductive doped phase II. Once again, the 33 mol% eutectic composition has the highest conductivity in this region, probably as a result of the low liquidus temperature.

Phase I region. The temperature range in which Phase I of P_{12}TFSA is stable also coincides with the region where the liquid phase is present for samples with LiTFSA contents greater than around 9 mol%. In this case the presence of liquid is clearly recognizable by the slope $d\ln\sigma/d(1/T)$. Up to approximately 5 mol% Li^+, a sudden upturn of the conductivity is seen as the liquidus temperature is approached, in sharp contrast to samples with Li^+ concentration >9.3 mol%, where $d\ln\sigma/d(1/T)$ is practically constant before the conductivity almost levels off beyond the final liquidus temperature. This provides us with some additional evidence that, for compositions between 0 and approximately 5 mol% LiTFSA, phase I is a solid phase, albeit with a great degree of translational and rotational mobility which produces a fast ion conductive solid phase. The lithium solid state NMR spectra discussed above confirm that the lithium ion is indeed liquid like in its transport properties and hence is at least a contributor to this fast ion conduction. Of course the ^{1}H solid state NMR of related plastic crystal compounds discussed by Ono *et al.*[6–8] suggest that there will be also significant P_{12} cation transport in this phase, and indeed some of our own preliminary ^{1}H diffusion work in these systems[23] shows that at least some fraction of the cations are showing significant diffusivity. However, based on the conductivity of the pure compound, it is unlikely that the almost four orders of magnitude increase in conductivity between 0 and 5 mol% Li^+ can be due to changes in the P_{12} cation diffusivity. A plausible description of the observed fast ion conduction is therefore that the lithium ion is the primary

diffusing species, and that its motion is facilitated by the rotation of the matrix cation (and/or anion), similar to the process discussed by Cooper and Angell for the Li_2SO_4 and $LiBF_4$ doped tetraalkylammonium systems.[1,5]

Conclusions

Thermal analysis and NMR spectroscopy support the hypothesis that lithium ions are soluble in the highest temperature phase of the P_{12}TFSA compound, up to approximately 5 mol%. Conductivity in these doped systems is very significantly higher than the pure P_{12}TFSA compound. Combined with ^{7}Li NMR linewidth measurements, lithium fast-ion conduction is indicated. A eutectic composition was also apparent in this mixed system with a melting point of approximately 308 K. The eutectic composition displayed the highest conductivity over the entire temperature range examined.

References

1 E. I. Cooper and C. A. Angell, *Solid State Ionics*, 1984, **18-19**, 570.
2 F. Gray *Polymer Electrolytes- Fundamentals and Applications*, VCH, New York, 1991.
3 J. Timmermans, *J. Phys. Chem. Solids*, 1961, **18**, 1; T. Atake and C. A. Angell, *J. Phys. Chem.*, 1979, **83**(25), 3218.
4 J. M. Chezeau and J. H. Strange, *Physics Reports (Review Section of Physics Letters)*, 1979, **53**(1), 1–92.
5 R. Aronsson, H. E. G. Knape and L. M. Torell, *J. Chem. Phys.*, 1982, **77**(2), 677.
6 H. Ono, S. Ishimaru, R. Ikeda and H. Ishida, *Bull. Chem. Soc. Jpn.*, 1999, **72**, 2049.
7 H. Ono, S. Ishimaru and R. Ikeda, *Ber. Bunsenges. Phys. Chem.*, 1998, **102**, 650.
8 H. Ono and R. Ikeda, *Ber. Bunsenges. Phys. Chem.*, 1996, **100**, 1833.
9 T. Shimizu, S. Tanaka, N. Onoda-Yamamuro, S. Ishimaru and R. Ikeda, *J. Chem. Soc., Faraday Trans.*, 1997, **93**(2), 321.
10 (*a*) M. Hattori, S. Fukada, D. Nakamura and R. Ikeda, *J. Chem. Soc., Faraday Trans.*, 1990, **86**, 3777; (*b*) S. Iwai, M. Hattori, D. Nakamura and R. Ikeda, *J. Chem. Soc., Faraday Trans.*, 1993, **89**, 827; (*c*) H. Ishida, Y. Furukawa, S. Kashino, S. Sato and R. Ikeda, *Ber. Bunsenges. Phys. Chem.*, 1996, **100**, 433; (*d*) T. Tanabe, D. Nakamura and R. Ikeda, *J. Chem. Soc., Faraday Trans.*, 1991, **87**(7), 987.
11 (*a*) J. Sun, D. R. MacFarlane and M. Forsyth, *Ionics*, 1997, **13**, 356; (*b*) J. Sun, D. R. MacFarlane and M. Forsyth, *J. Phys. Chem. B*, 1998, **102**(44), 8858.
12 D. R. MacFarlane, J. Huang and M. Forsyth, *Nature (London)*, 1999, **402**, 792.
13 D. R. MacFarlane, P. Meakin, J. Sun, N. Amini and M. Forsyth, *J. Phys. Chem.*, 1999, **103**, 4164.
14 J. Huang, D. R. MacFarlane and M. Forsyth, *Solid State Ionics*, in the press.
15 O. A. Porter and K. E. Easterling *Phase Transformations in Metals and Alloys*, 2nd edn., Chapman & Hall, London, UK, 1992.
16 A. Noda, A. Nishimoto and M. Watanable *The Sixth International Symposium on Polymer Electrolytes, Extended Abstracts*, Hayama, Japan, 1998, p. 54.
17 P. E. Stalworth, S. G. Greenbaum, F. Croce, S. Slane and M. Solomon, *Electrochim. Acta*, 1995, **40**, 2137.
18 H. Every, F. Zhou, M. Forsyth and D. R. MacFarlane, *Electrochim. Acta*, 1998, **43**, 1465.
19 A. Ferry, L. Edman, M. Forsyth, D. R. MacFarlane and J. Sun, *Electrochim. Acta*, 2000, **45**, 1237.
20 F. Ali, M. Forsyth, M. C. Garcia, M. E. Smith and J. H. Strange, *Solid State Nucl. Magn. Reson.*, 1995, **5**, 217.
21 S. Ng, M. Forsyth, D. R. MacFarlane, M. Garcia, M. E. Smith and J. H. Strange, *Polymer*, 1998, **39**, 6261.
22 A. Abragam, *Principles of Nuclear Magnetism*, Oxford Science Publications, New York, 1996, p. 2.
23 H. Every and M. Forsyth, unpublished work. .